Communications and Network, 2022, 14, 91-107
https://www.scirp.org/journal/cn
ISSN Online: 1947-3826
ISSN Print: 1949-2421

Comparing the Performances between Adaptive Notch Filter Direct and Lattice Forms Structures for Mitigation Jamming Signals

Abdelrahman El Gebali, René Jr Landry

Lassena Laboratory, Department of Electrical Engineering, École de Technologie Supérieure (ÉTS), Montreal, Canada
Email: abdelrahman.elgebali@lassena.etsmtl.ca

How to cite this paper: El Gebali, A. and Landry, R.J. (2022) Comparing the Performances between Adaptive Notch Filter Direct and Lattice Forms Structures for Mitigation Jamming Signals. *Communications and Network*, **14**, 91-107.
https://doi.org/10.4236/cn.2022.143007

Received: May 12, 2022
Accepted: July 3, 2022
Published: July 6, 2022

Abstract

A jamming signal such as single and multiple Continuous-Wave (CW and MCW) interferences have been shown to have severe effects on the quality of the received signal in wireless communication. This paper presents an approach of a low-complexity algorithm that compares the performances of using Adaptive Notch Filter (ANF) direct and lattice forms structures based on second-order Infinite Impulse Response (IIR) Notch Filter (NF) for the detection and mitigation of CW and MCW interferences in QPSK communication systems. The approach method consists of two ANFs, adaptive IIR NF $H_{d_1,l_1}(z)$ and adaptive IIR NF $H_{d_2,l_2}(z)$. The present algorithm can estimate and mitigate each CWI and computer their power in Time-Domain (TD). In results for performance comparison, the lattice IIR NF structure outperforms the direct IIR NF structure for detection and removal jamming and has a better Bit Error Ratio (BER). Furthermore, compared with the case of full suppression ($k_1 = 1$), both cases (direct and lattice form) work better for low and high-power jammers. Also, compared to the case without an IIR NF, the presented algorithm can detect and mitigate, track hopping frequency interference, and improve BER performance.

Keywords

CWI, MCWI, ANF, BER, IIR, QPSK, Direct and Lattice Form, and JSR

1. Introduction and Background

In many fields of telecommunications, particularly wireless communication, several existing techniques have been developed to mitigate the CWI and MCWI that impact the receiver end. However, wireless communication still suffers from the CWI and MCWI affecting the receiver, causing data distortion, and the receiver performance degraded, reducing 1) the Signals-of-Interest (SoI) quality, 2) degrading the Quality of Service (QoS), 3) increasing the BER 4)lowering the Signal-to-Noise Ratio (SNR).

In the literature, CWI and MCWI have been studied in various contexts. In the contexts of Wireless Sensor Networks (WSNs) [1] [2], Orthogonal Frequency Division Multiplexing (OFDM) communications [3], Multi-Hop Wireless Networks (MHWNs) [4], and Long-Term Evolution (LTE) cellular communications [5]. [6], discusses the negative effects of jamming on GNSS receiver performance and introduces three types of jamming detection: digital pre-correlation signal processing, post-correlation domain, and Automatic Gain Control (AGC). In GNSS signals [7], interference can be easily detected and mitigated because of the large distance between transmitter and receiver.

At present, different kinds of methods can be employed at the receiver end for interference detection and mitigation in radio frequency (RF) communications, which can be classified into several approaches such as TD, Frequency Domain (FD), and space domain (antenna array). Antenna arrays with adaptive beamforming are used in space domain approaches to suppress interfering signals by directing the beam in different directions or placing nulls in the interfering signal's path [8] [9]. [10] proposed a cascaded interference and multipath suppression method using an array antenna. Also, the antenna array model was proposed for interference multipath [11]. However, the major drawback of these methods is high computational complexity and incurred hardware. In FD, several mitigation methods have been proposed for removing the Jamming signal. The hardware complexity of requiring Fast Fourier transform (FFT), inverse FFT, and the high cost is a major limitations for FD [12] [13] [14]. Therefore, TD techniques (adaptive filter) have attracted considerable attention to solutions for the detection and mitigation of CWI because it has less hardware complexity. The TD techniques adopt ANF methods by using either the FIR or the IIR. In literature, the adaptive lattice IIR NF and adaptive direct IIR NF have been widely used, studied, and analyzed [15] [16] [17] [18]. Their applications are found in various digital signal processing applications such as communication, sonar, radar, biomedical engineering, control, etc. The notch filter is widely used to cancel unwanted frequencies in various fields [14]. In [15] [16], the authors have presented simple techniques for detecting and mitigating CWI using an adaptive lattice IIR NF. [19] proposed ANF to estimate the existence of CWI in GNSS. The ANF based on lattice form is used to detect the CWI as in [20]. [21] present an enhanced nonlinear prediction method for mitigating interference. [22] proposed a new method for rejecting the CWI in the Global Positioning System (GPS) based on cascading an adaptive FIR filter and Wavelet Packet Transform (WPT) based filter. [23] proposed IIR ANF to cancel the jamming effect on the received GPS signal. The authors [24] proposed an anti-jamming filter to reduce the CWI based on the second-order IIR Notch Filter. [25] proposed an anti-jamming technique based on a lattice NF that is fully adaptive.

Adaptive Notch Filters (ANFs) are utilized to eliminate or reduce CW and MCW interferences in various signal processing applications such as biomedical [26] [27], communication, and GNSS applications [20] [28], radar, control, and other related areas. ANF is performed using the Finite Impulse Response (FIR) and the Infinite Impulse Response (IIR), which are the two types of Adaptive Digital Notch Filters (ADNFs) that are most common. In addition, because IIR requires less computation, IIR is more widely used than FIR [29]. The IIR NF can effectively remove the CWI or NBI [30].

A typical IIR NF has constrained zero on a unit circle with a phase equal. The notch depth becomes infinite as an outcome, allowing the CWI to be removed completely. However, since the CWI is totally eliminated, this approach yields a significant amount of self-noise [31], which is briefly described in [32]. A deep notch is required for high-power jammers cases for optimal jamming removal.

Several approaches have been written in the literature to determine efficient NF implementation structure, adaptation algorithm, and the rejection or mitigation of CW and MCW interference [33] [34] [35] [36] [37]. However, most of them were not focused on adjusting the notch depth and did not include the comparison between direct and lattice IIR NF form structures.

This paper presents a low-complexity algorithm TD approach for general wireless communications. It aims to determine the efficiency of the adaptive NF implementation on direct and lattice forms structures for mitigation interferences by considering adjusting the notch depth and then comparing the performances between the two types of structures: direct and lattice, and considering which one should be chosen for practical applications.

The rest of this paper is divided into five sections: Section 2 describes the adaptive direct IIR NF and adaptive lattice IIR NF and received signal model. The proposed mitigation method using adaptive IIR NF and its adaptation algorithm is introduced in Section 3. Simulation results and discussion of the comparing performances of two structures are demonstrated in Section 4. Last, Section 5 concludes the paper.

2. Adaptive IIR Notch Filter

Digital filters are the most widely used in communication areas. There are two major implementations of an Adaptive Notch Filter (ANF), which are the Finite Impulse Response (FIR), and the Infinite Impulse Response (IIR). FIR filters are also called the Moving Average (MA) filters that implement an all-zero transfer function. While the Auto-Regression (AR) and the MA, or an ARMA, commonly realize an IIR filter that implements all poles and zeroes transfer function. The adaptive filter can be performed in several various structures or realizations. The chosen structure can affect the process's computational complexity and the number of iterations required to achieve the desired performance level.

ANF is widely used to detect and mitigate unwanted signals in signal processing applications. It has two forms of structure: direct and lattice [15]. This section introduces both ANF structures, as are presented below.

Direct IIR NF

The transfer function $H_{d1}(z)$ of the second-order adaptive direct IIR NF is given by [28]

$$H_{d1}(z) = \frac{N_{d1}(z)}{D_{d1}(z)} = \frac{1 + k_{od} Z^{-1} + Z^{-2}}{1 + \beta k_{od} Z^{-1} + \beta^2 Z^{-2}} \tag{1}$$

Lattice IIR NF

The transfer function $H_{l1}(z)$ of the second-order adaptive lattice IIR NF is expressed [16] as

$$H_{l1}(z) = \frac{N_l(z)}{D_l(z)} = \frac{1 + 2k_{ol} Z^{-1} + Z^{-2}}{1 + k_{ol}(1+\beta) Z^{-1} + \beta Z^{-2}} \tag{2}$$

where subscripts d and l denote the direct and lattice form structures, respectively, β is the pole radius that controls the bandwidth of NF, which is over (0, 1) to ensure the stability of NF, and k_{od} and k_{ol} are the notch coefficient parameter whose true value is defined by $-2\cos(\omega_o)$ and $-\cos(\omega_o)$. ω_o is the frequency of jamming signal. The larger β, the narrower the bandwidth of NF is. If the absolute values of β and k_{od} and k_{ol} are less than one then the $H_{d1}(z)$ and the $H_{l1}(z)$ are stable.

Received Signal Model and Jamming Signal

- Received signal

Let us consider the adaptive algorithm that attempts to adjust, k_{od} and k_{ol} in Equation (1) and Equation (2) of the IIR NF. It is assumed that the interferences signal (jamming) with the AWGN are added to the QPSK signal, as expressed in Equation (3), where $r(n)$ is the input signal to the ANF, as shown in Figure 1.

$$r(n) = S(n) + w(n) + J_i(n) \tag{3}$$

where $S(n)$, $w(n)$ and $J_i(n)$ are the QPSK modulated signal, represents AWGN and jamming signal, respectively.

- Jamming signal

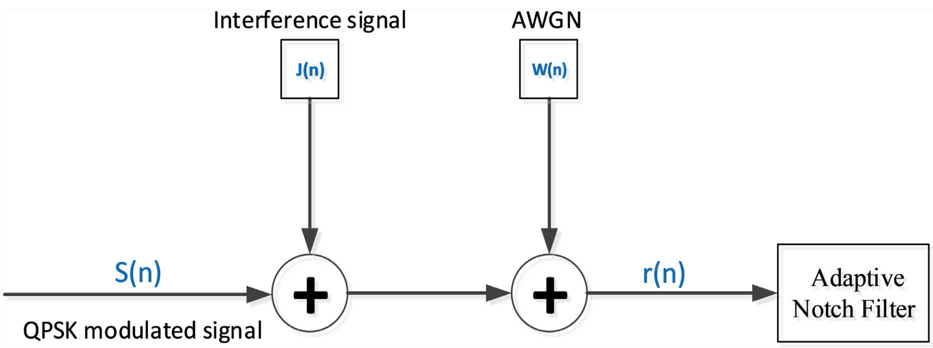

Figure 1. A system model of the received signal block diagram.

The jamming signal is assumed to be single and multiple continuous-wave interferences and can be expressed as:

$$J_i(n) = \sum_{i=1}^{m} A_i \cos(\omega_i n + \theta_i) \tag{4}$$

where

- A_i is the amplitude of the i^{th} jamming signal;
- ω_i is the frequency of the i^{th} interference signal and $\omega_i = 2\pi f_i$;
- θ_i is the phase delay of the i^{th} jamming signal, uniformly distributed in the range $[-\pi, \pi]$;
- m is the number of jamming, and n is the time index.

Substituting Equation (4) into Equation (3), then the received signal becomes:

$$r(n) = S(n) + w(n) + \sum_{i=1}^{m} A_i \cos(2\pi f_i n + \theta_i) \tag{5}$$

3. Proposed Mitigation Method Using Adaptive IIR NF

For perfect CWI and MCWI removal for high-power jammers cases, as previously stated, a deep notch is required. ANFs, on the other hand, introduce self-noise, increasing the BER and reducing the SNR. As a result, the notch depth should be controlled and adjusted according to the power of the interference (JSR) to reduce self-noise. Therefore, this section introduces the mitigation method for CWI and MCWI. The mitigation method consists of two ANFs, the adaptive IIR NF $H_{d_1,l_1}(z)$ and the adaptive IIR NF $H_{d_2,l_2}(z)$ as shown in Figure 2, where the ANF $H_{d_1,l_1}(z)$ is utilized to detect and estimate the frequency of the interference (ω_o) and JSR, respectively and the ANF $H_{d_2,l_2}(z)$ is used to mitigate the interference.

In this paper, the mitigation method shown in Figure 2 will be used to mitigate the CWI, which uses Single-Adaptive IIR NF (S-ANF) model. The S-ANF model consists of two ANFs, the adaptive IIR NF $H_{d_1,l_1}(z)$ and the adaptive IIR NF $H_{d_2,l_2}(z)$ as shown in Figure 2. The ANF $H_{d_1,l_1}(z)$ is employed to detect and estimate the interference frequency (ω_o) and then calculated JSR whereas the ANF $H_{d_2,l_2}(z)$ is used to mitigate the interference. In contrast, the mitigation method shown in Figure 3 will be used to mitigate the MCWI, which uses the Multiple Adaptive IIR Notch Filter (MANF) models. Each stage of the

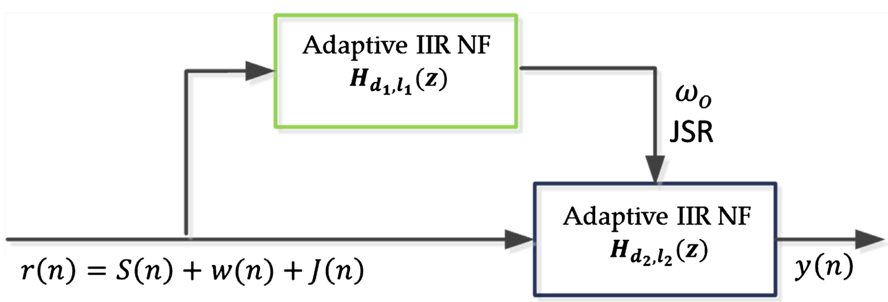

Figure 2. Block diagram of the mitigation method of a system model.

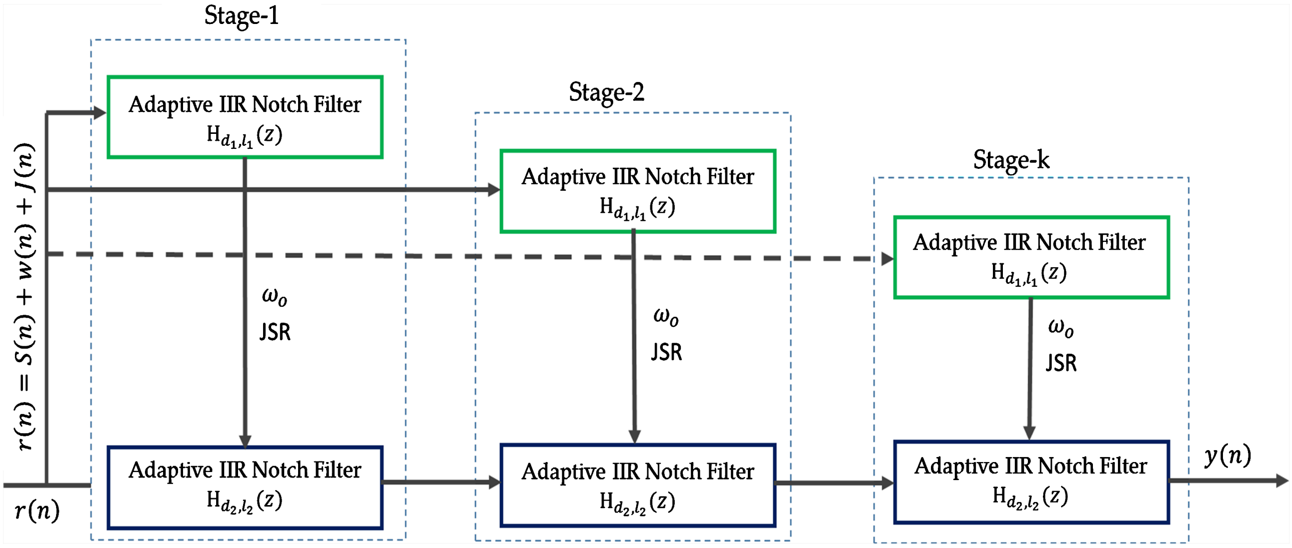

Figure 3. The mitigation system model of the MANF block diagram.

MANF model has two ANFs. The same structure that was used to mitigate CWI can be used to implement the structure of each stage.

3.1. Adaptation Algorithms

The output signals of the filters [$H_{d1}(z)$ and $H_{l1}(z)$] as described in Equation (1) and Equation (2), are respectively expressed as

$$y_d(n) = x(n) + k_{od}x(n-1) + x(n-2) - \beta k_{od}y(n-1) - \beta^2 y(n-2) \quad (6)$$

and

$$y_l(n) = u(n) + 2k_{ol}u(n-1) + u(n-2) \quad (7)$$

where

$$u(n) = r(n) - k_{ol}(1+\beta)u(n-1) - \beta u(n-2) \quad (8)$$

The adaptive algorithms to control the update filter coefficient for direct and lattice form structures, respectively, are given by [18] [38].

$$k_{od}(n+1) = k_{od}(n) - \mu y(n)\left(g_d\left(J\left(k_{od}\right)\right)\right) \quad (9)$$

and

$$k_{ol}(n+1) = k_{ol}(n) - \mu y(n)\left(g_l\left(J\left(k_{ol}\right)\right)\right) \quad (10)$$

where $g_d\left(J\left(k_{od}\right)\right)$ and $g_l\left(J\left(k_{ol}\right)\right)$, the gradient signal of direct and lattice IIR NF, respectively, and given by [18] [38]:

$$g_d\left(J\left(k_{od}\right)\right) = x(n-1) - \beta y(n-1) \quad (11)$$

and

$$g_l\left(J\left(k_{ol}\right)\right) = -(1+\beta)u(n-1) \quad (12)$$

Then after substituting Equation (11) into Equation (9) and Equation (12) into Equation (10), Equations (9)-(10) become

$$k_{od}(n+1) = k_{od}(n) - \mu y(n)\big(x(n-1) - \beta y(n-1)\big) \quad (13)$$

$$k_{ol}(n+1) = k_{ol}(n) - \mu y(n)\big((1-\beta)u(n-1)\big) \quad (14)$$

Equation (13) and Equation (14) are the adaptive algorithms for direct and lattice IIR NF structure, respectively, that control the update coefficient of the filter. μ is the step size and parameter that controls the convergence speed.

Since the normalized notch frequencies (f_{Nd}, f_{Nl}) and the notch parameter (k_{od}, k_{ol}) are related by $k_{od} = -2\cos(\omega_{od})$, and $k_{ol} = -\cos(\omega_{ol})$, where $\omega_{od} = 2\pi f_{Nd}$ and $\omega_{ol} = 2\pi f_{Nl}$, at sample *n*, the estimated frequency is given by:

$$\hat{f}_{Nd}(n) = \frac{1}{2\pi}\cos^{-1}\big(-0.5k_{od}(n)\big) \quad (15)$$

$$\hat{f}_{Nl}(n) = \frac{1}{2\pi}\arccos\big(\hat{k}_{ol}(n)\big) \quad (16)$$

3.2. Mitigating CW Interfering Signal

Adaptive direct and lattice IIR NF is utilized to mitigate the CW interfering signal, whose transfer function $H_{d2}(z)$ and $H_{l2}(z)$, respectively, as is given [16] [18] [38]

$$H_{d2}(z) = \frac{N_{d2}(z)}{D_{d2}(z)} = \frac{1 + k_{0d}(k_1)Z^{-1} + k_1 Z^{-2}}{1 + k_{0d}(\beta k_1)Z^{-1} + \beta^2 k_1 Z^{-2}} \quad (17)$$

and

$$H_{l2}(z) = \frac{N_{l2}(z)}{D_{l2}(z)} = \frac{1 + k_{0l}(1+k_1)Z^{-1} + k_1 Z^{-2}}{1 + k_{0l}(1+\beta k_1)Z^{-1} + \beta k_1 Z^{-2}} \quad (18)$$

where k_1, the notch depth and dependents on the estimated JSR. β, the pole radius of the IIR NF that determines the width, as seen in **Figure 4** and **Figure 5**. As previously indicated, several implementation techniques can be obtained $H_{d2}(z)$ and $H_{l2}(z)$. In this work, the transfer function of $H_{d2}(z)$ and $H_{l2}(z)$ implement by cascading all-pole and all-zero IIR NF. Setting $k_1 = 1$ resulting in $H_{d2}(z) \equiv H_{d1}(z)$ and $H_{l2}(z) \equiv H_{l1}(z)$ [16] [18]. Hence, same structure can be used to implement the $H_{d2}(z)$ and $H_{l2}(z)$. By copying K_{0d} of the $H_{d1}(z)$ and K_{0l} of the $H_{l1}(z)$ that is tuned to the IF by Equation (13) and Equation (14), the notch of Equation (18) and Equation (19) can be placed on the IF. As seen in **Figure 5**, the amount of reduction is dependent on the depth of the notch. In the case of $k_1 = 1$, the $H_{d2}(z)$ and $H_{l2}(z)$ are the same as $H_{d1}(z)$ and $H_{l1}(z)$, respectively which has zero on the unit circle and infinite depth of the notch, removing all interference caused by excluding some useful signals. Hence, to reduce signal distortion, the depth of the notch k_1 should be adjusted with respect to the JSR estimated. The parameters JSR, the notch parameter (k_{od}, k_{ol}) and the notch depth (k_1) are required when designing $H_{d2}(z)$ and $H_{l2}(z)$.

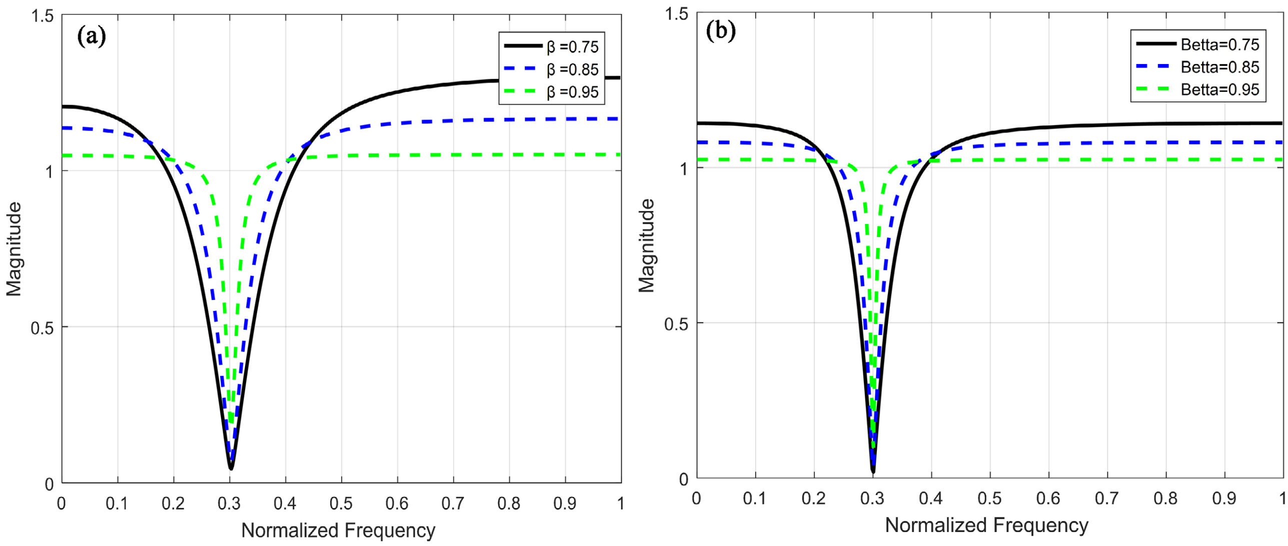

Figure 4. The notch characteristics concerning filter parameters; Notch width vs. β: (a) Direct form, (b) Lattice form.

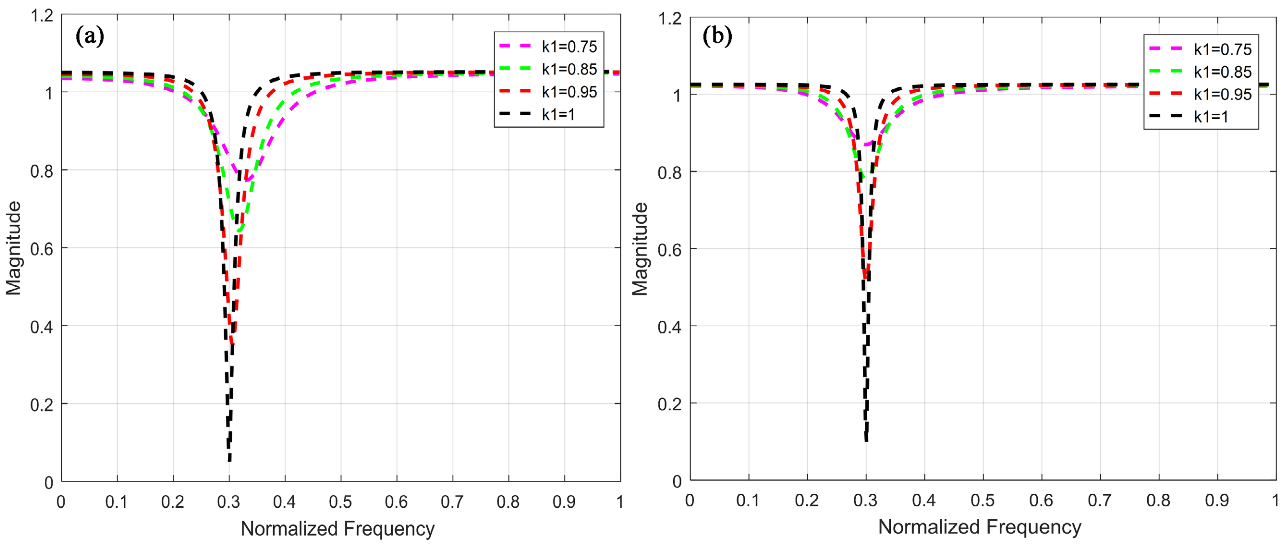

Figure 5. The notch characteristics concerning filter parameters; Notch depth vs. k_1: (a) Direct form, (b) Lattice form.

The SNR output of the second-order IIR NF is expressed as a function of its parameter to obtain the optimal value of the parameter that controls the depth [15] [16].

$$SNR_o dB = 10\log_{10}\left(\frac{E\left[S^2(n)\right]}{E\left[\left(y(n)-S(n)\right)^2\right]}\right) \tag{19}$$

where $y(n)$, the output of the 2nd IIR NF $H_{d2}(z)$ and $H_{l2}(z)$, which expressed as:

$$y(n) = y_d(n) = H_{d2}(z)r(n) \triangleq S_o(n) + w_o(n) + J_o(n) \tag{20}$$

and

$$y(n) = y_l(n) = H_{l2}(z)r(n) \triangleq S_o(n) + w_o(n) + J_o(n) \tag{21}$$

where $S_o(n)$, $w_o(n)$ and $J_o(n)$ respectively, are the output components of the desired QPSK modulated signal, the AWGN, and the CWI. $S_o(n)$ is a distorted version of the information signal $S(n)$ caused by information removal at the notch frequency of $H_{d2}(z)$ and $H_{l2}(z)$.

Equation (22) and Equation (23) describes $SNR_{od}dB$ *and* SNR_{ol} in terms of the filter parameters for direct and lattice form structure IIR NF, respectively, are given by [16] [18]:

$$SNR_{od}dB = 10\log_{10}\left(\frac{1}{\left(1+\sigma^2\right)\left(\dfrac{1+k_1^2-2\beta^2k_1^2}{\left(1-\beta^2k_1^2\right)}\right)+JSR_i\left(\dfrac{\left(1-k_1\right)^2}{\left(1-\beta k_1\right)^2}\right)-1}\right) \tag{22}$$

and

$$SNR_{ol} = \frac{1}{\left(1+\sigma^2\right)\left(\dfrac{\left(1+k_1^2-2\beta k_1^2\right)}{1-\beta^2k_1^2}\right)+JSR_l\left(\dfrac{\left(1-k_1\right)^2}{\left(1-\beta k_1\right)^2}\right)-1} \tag{23}$$

where σ^2 is the variance of AWGN, and $JSR_i = \frac{A_i^2}{2}$.

To maximize $SNR_o dB$ in Equation (22) and Equation (23), the optimal value (k_1) needs to be found by minimizing the denominator of Equation (22) and Equation (23), then the denominator can be rewritten as a function of k_1

$$f\left(k_1\right) = \left(\frac{1+k_1^2-2\beta^2k_1^2}{1-\beta^2k_1^2}\right)+G_i\left(\frac{\left(1-k_1\right)^2}{\left(1-\beta^2k_1\right)^2}\right)-\frac{1}{1+\sigma^2} \tag{24}$$

and

$$f\left(k_1\right) = \left(\frac{1+k_1^2-2\beta k_1^2}{1-\beta^2k_1^2}\right)+G_l\left(\frac{\left(1-k_1\right)^2}{\left(1-\beta k_1\right)^2}\right)-\frac{1}{1+\sigma^2} \tag{25}$$

where $G_i = \frac{JSR_i}{1+\sigma^2}$.

We differentiate $f\left(k_1\right)$ and solve $f'\left(k_1\right)=0$ for all possible roots of k_1, Equation (24) and Equation (25) has at least one real root in the [0 1] range that gives the optimal k_1 as a function of JSR_i. **Figure 6** shows the optimal k_1 as a function of JSR. As the JSR increases, we can see that k_1 approaches 1 for both the direct IIR NF and lattice IIR NF. However, for the lattice, k_1 approaches 1 faster than in the direct at the same E_b/N_o parameters.

4. Simulation Results for Performance Comparison and Discussion

This section discusses the performance comparison between the direct IIR NF forms structure and lattice IIR NF forms structure. The approach algorithm is employed to remove and excise the CWI and MCWI from QPSK signals. ANF direct and lattice approach has been utilized to control the update coefficient of filter and notch depth. The BER is used to evaluate the system performance of the approach algorithm for varying JSR and E_b/N_o. In this work, the jamming signal is considered to be CWI and MCWI, with unknown amplitude (A_i). The center frequencies ($f_1 = 0.03$ and $f_2 = 0.08$) and β is chosen to 0.98 to provide more acceptable outcomes in various scenarios. A large β value gave slower convergence and tracking but more accurate frequency estimates and JSR [15] in ANF $H_{d1}(z)$. The BER is quantified in terms of E_b/N_o changes and JSR changes. All simulation results were obtained using MATLAB® Software.

Figure 7 shows the performance comparing the two cases, direct and lattice

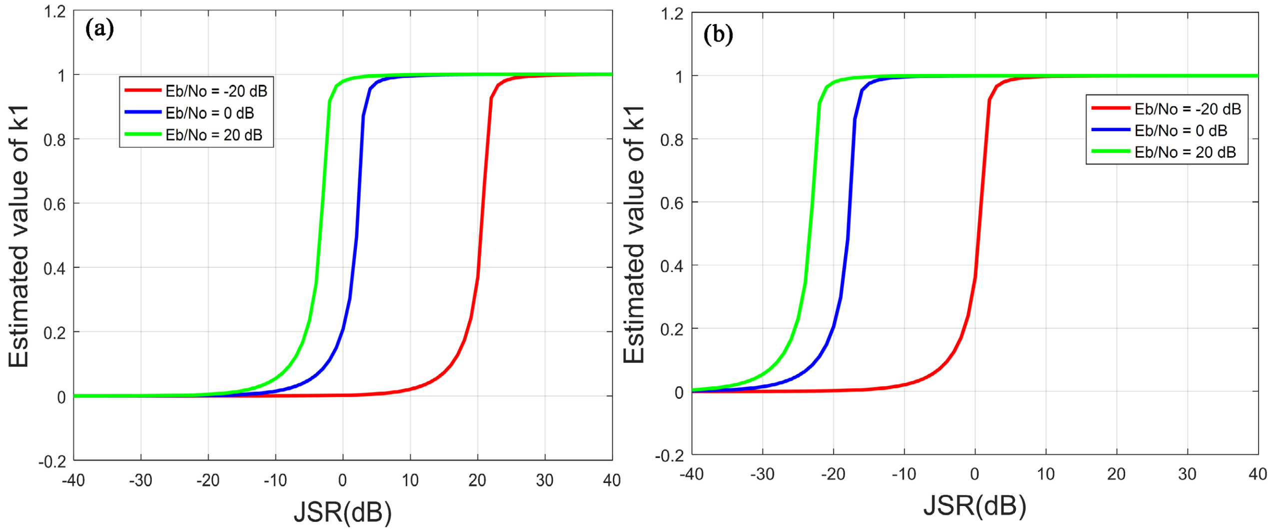

Figure 6. The estimated optimal k_1 vs. JSR: (a) Direct form, (b) Lattice form.

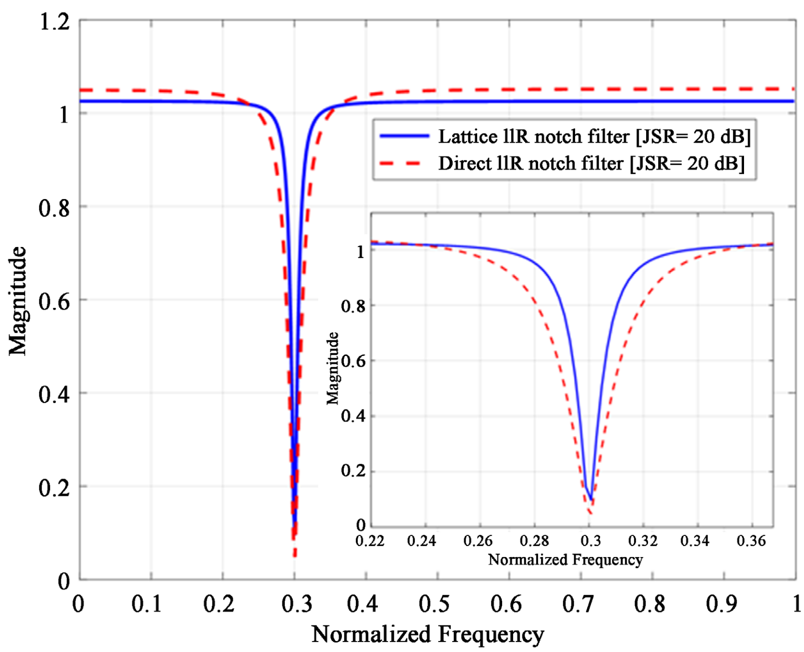

Figure 7. Notch depth vs. JSR.

IIR NF using the same JSR. The result shows that the direct IIR NF has a deeper notch and wide bandwidth than lattice IIR NF; this means that lattice IIR NF is more stable and has an accurate frequency estimate than direct IIR NF.

The Figures below depict the BER performance as E_b/N_o changes. Simulations results were done with a constant value of JSR and various values of E_b/N_o. Figure 8 and Figure 9 illustrate the BER performance by controlling the depth of the NF for both the direct and lattice IIR NFs in the presence of CW and MCW interferences. The results demonstrate that the simulations with lattice IIR NF achieve a better BER than in the case of the simulations with direct IIR NF, particularly when the JSR is small or large. Thus, the ANF in both cases, direct and lattice IIR NF, can reduce interferences and obtain a better BER than

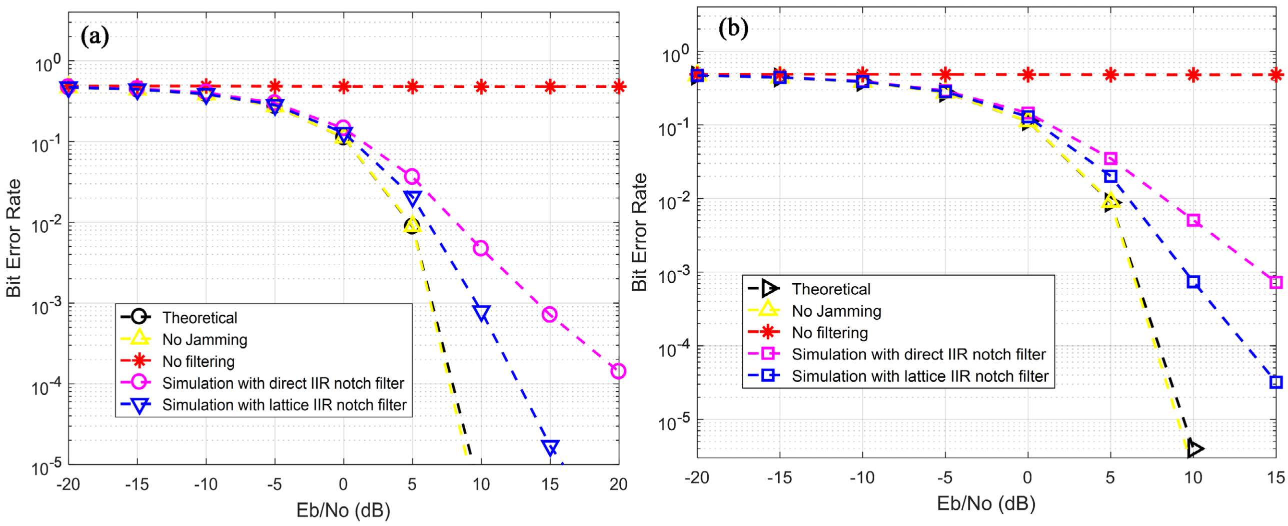

Figure 8. BER vs. $\frac{E_b}{N_o}$ of QPSK in the presence of CWI: (a) JSR = −12 dB, (b) JSR = 10 dB.

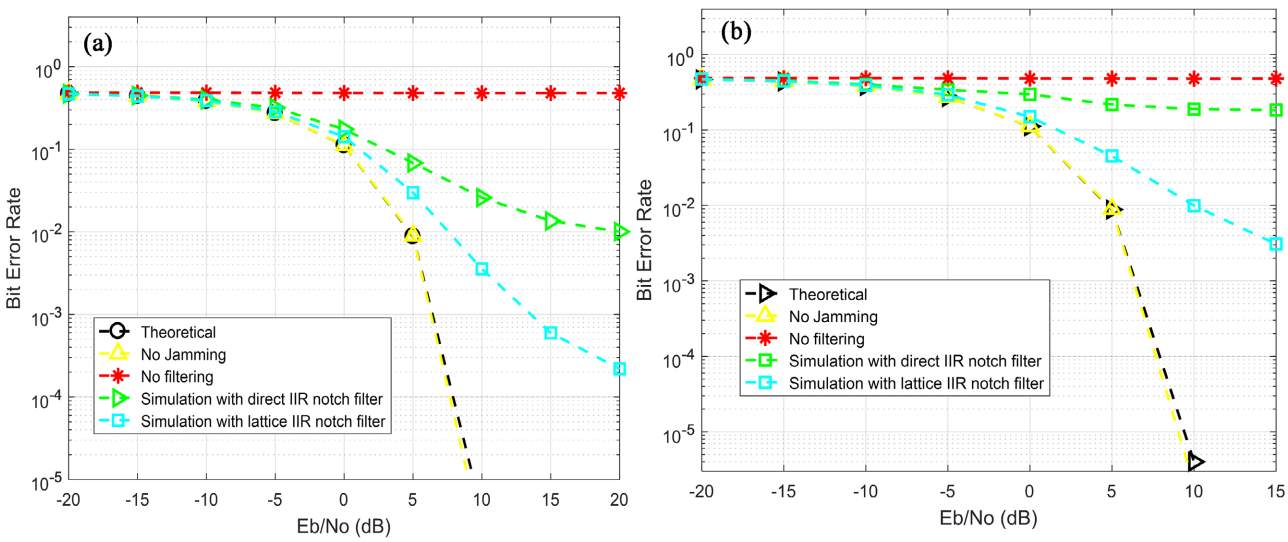

Figure 9. BER vs. $\frac{E_b}{N_o}$ of QPSK in the presence of MCWI: (a) JSR = −12 dB, (b) JSR = 10 dB.

the case with no filtering. Moreover, lattice IIR NF performs better than direct IIR NF.

The performance of BER with variations of the JSR is shown in Figure 10 and Figure 11. Simulations were carried out with a constant E_b/N_o value and by adjusting the depth of the NF. Also, results were compared between the two cases of direct IIR NF and lattice IIR NF (filtering) and also with the case of no filtering. Therefore, the simulation results show that both cases of direct IIR NF and lattice IIR NF outperform the no filtering in case of filtering. Moreover, lattice IIR NF outperforms direct IIR NF while using a Single-Adaptive IIR NF (S-ANF) and Multiple Adaptive IIR NF (MANF). The lattice IIR NF algorithm efficiently controlled the notch depth and achieved better results than the direct

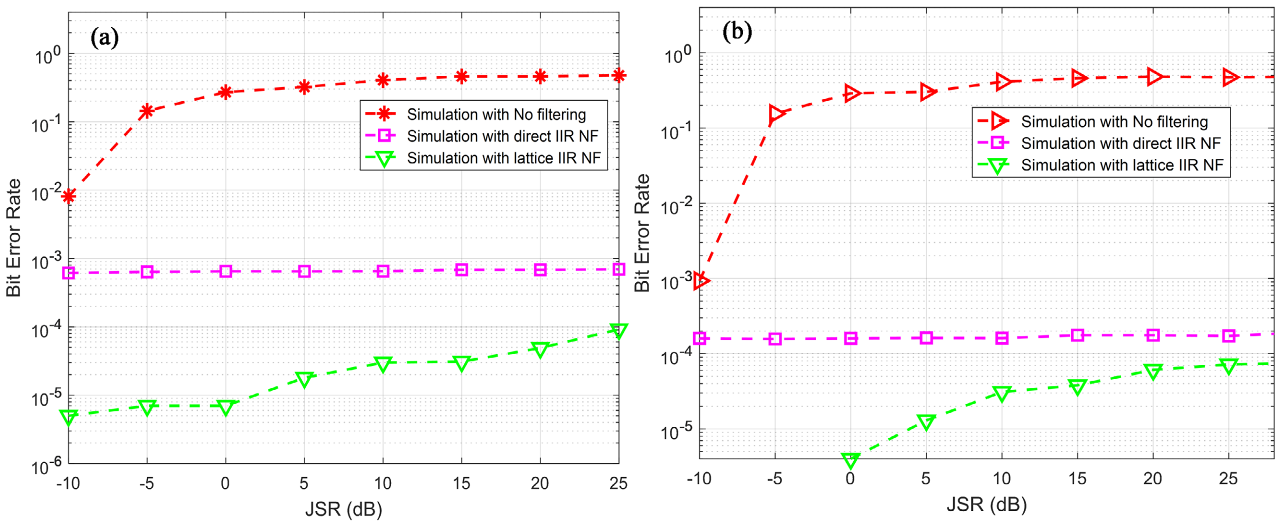

Figure 10. BER vs. JSR using S-ANF: (a) $\frac{E_b}{N_o} = 15\text{ dB}$, (b) $\frac{E_b}{N_o} = 20\text{ dB}$.

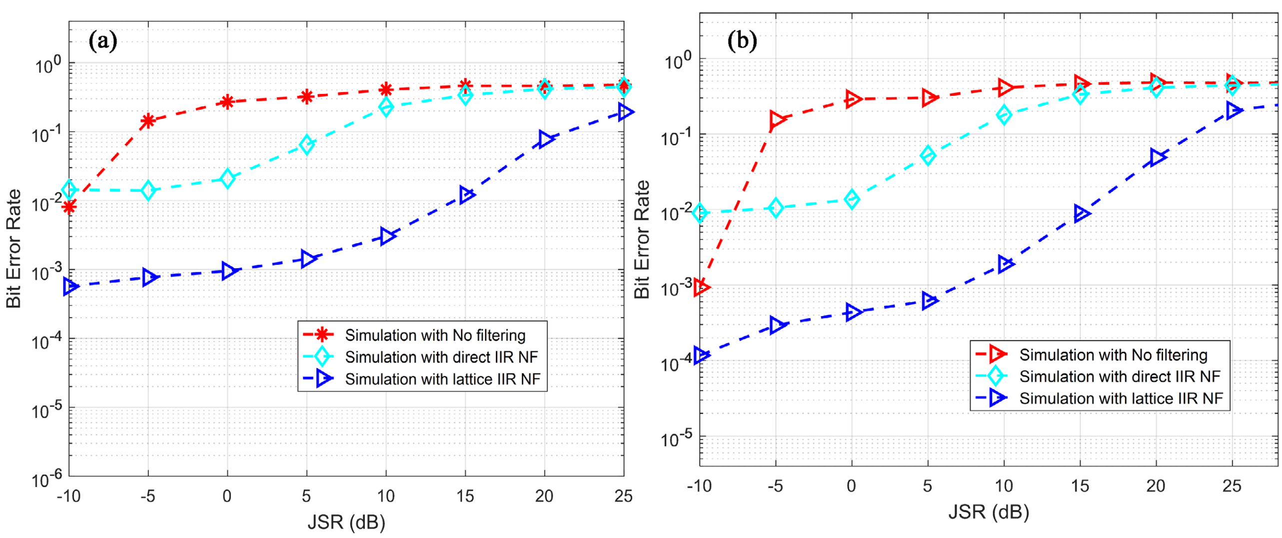

Figure 11. BER vs. JSR using MANF: (a) $\frac{E_b}{N_o} = 15\text{ dB}$, (b) $\frac{E_b}{N_o} = 20\text{ dB}$.

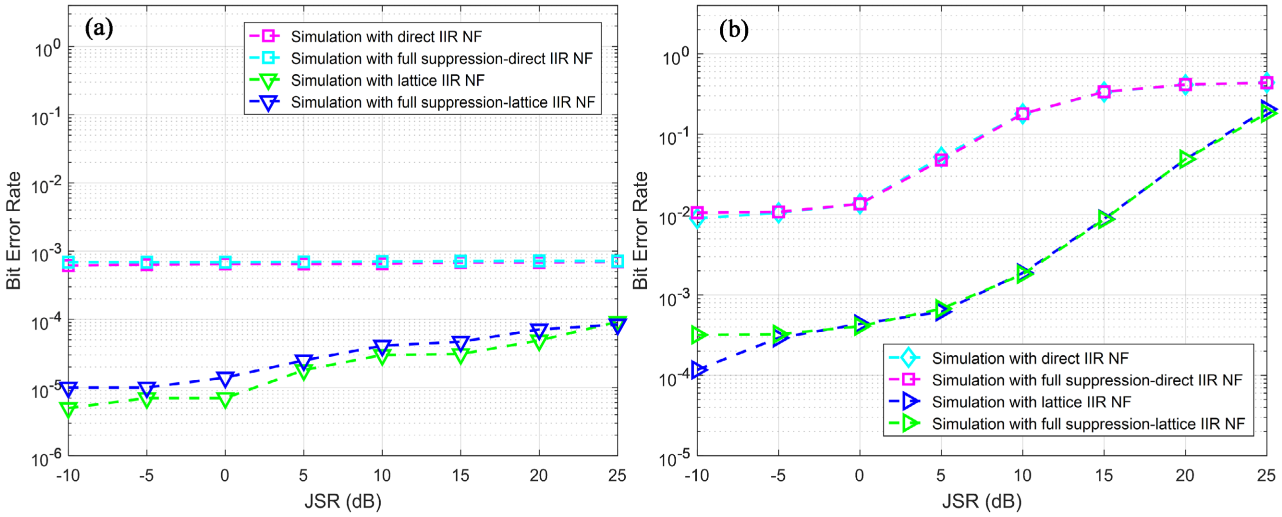

Figure 12. BER vs. JSR: (a) $\frac{E_b}{N_o} = 15$ dB, full suppression ($k_1 = 1$) using S-ANF, (b) $\frac{E_b}{N_o} = 20$ dB full suppression($k_1 = 1$) using MANF.

IIR NF algorithm. Figure 12 illustrates that the lattice and direct IIR NF outperform full suppression ($k_1 = 1$).

Most of the previous studies discussed in this paper focused on mitigation jamming without comparing the direct and lattice IIR NF structures' performance by adjusting the notch depth. These approaches totally eliminate jamming, but they generate a self-noise, which causes distortion and loss of some useful signals. To limit the loss and distortion of useful signals while eliminating jamming, we present a low-complexity algorithm approach for both direct and lattice IIR NF forms structure based on a second-order NF to mitigate CW and MCW interferences and adjust notch depth and compare between two structures, which has not been studied in previous works—particularly [18] [36] [37] [38]. Furthermore, based on the comparison of the two structures and the results derived by MATLAB® Simulation, we observed that the lattice IIR NF structure achieves better performance than the direct IIR NF structure for detecting and removing jamming. For example, at E_b/N_o value of 15 dB in the presence of CWI with JSR = −12 dB, as seen in Figure 8, the BER of lattice IIR NF is 1.7e−5 compared to direct IIR NF, which is 5.9e−4. Also, as seen in Figure 9, in the presence of MCWI with the same jamming power, the BER of the lattice IIR NF is 6e−4 compared to the direct IIR NF, which is 1.3e−3. As a result, the lattice IIR NF has better BER performance than direct IIR NF in the presence of CWI and MCWI. Furthermore, by comparing the two cases, direct IIR NF and lattice IIR NF (filtering) with each other and with the case of no filtering. For example, at JSR = 5 dB using S-ANF, the BER of lattice IIR NF is 1.8e−5 while direct IIR NF is 6.5e−4, as seen in Figure 10, and also when using MANF, lattice IIR NF is 1.4e−3 while direct IIR NF is 6.4e−2, as shown in Figure 11. Thus, Lattice IIR NF outperforms direct IIR NF, and in the two cases, direct and lattice IIR NF outperform the no filtering case of filtering.

5. Conclusion

The paper presents the approach of a low-complexity algorithm for ANF based on second-order IIR NF, direct and lattice form structure for mitigation of CW and MCW interferences. It presents the performance comparison between the direct IIR NF forms structure and lattice IIR NF forms structure. Simulation results show that the BER performance of lattice IIR NF is better than direct IIR NF under both conditions (*in the presence of CWI and MCWI*). Also, the performance comparing the two cases of direct and lattice IIR NF with the case of no filtering show that both cases of direct and lattice IIR NF outperform the no filtering. Moreover, the lattice IIR NF outperforms direct IIR NF by using an S-ANF or MANF. It also observed that lattice IIR NF is more stable and accurate than direct IIR NF in estimating frequency, particularly in the low JSR. Both algorithms control the notch depth more efficiently, reduce interferences, and improve BER. Thus, lattice IIR NF is more suitable for practical applications than direct IIR NF. Therefore, this work can be applied to a DVB-S2 receiver or any other wireless communication receiver.

Acknowledgements

The work in this paper was done under the AVIO 601-Interference Mitigation in Satellite Communication Project of the LASSENA Lab, École de Technologie Supérieure (ÉTS). This research was also supported by the Natural Sciences and Engineering Research Council of Canada (NSERC), Thales, Telesat, Vigilant Global, CRIAQ, and Atem Canada.

Conflicts of Interest

The authors declare no conflicts of interest regarding the publication of this paper.

References

[1] Mpitziopoulos, A., Gavalas, D., Konstantopoulos, C. and Pantziou, G. (2009) A Survey on Jamming Attacks and Countermeasures in WSNs. *IEEE Communications Surveys & Tutorials*, **11**, 42-56. https://doi.org/10.1109/SURV.2009.090404

[2] Grover, K., Lim, A. and Yang, Q. (2014) Jamming and Anti-Jamming Techniques in Wireless Networks: A Survey. *International Journal of Ad Hoc and Ubiquitous Computing*, **17**, 197-215. https://doi.org/10.1504/IJAHUC.2014.066419

[3] Shahriar, C., *et al.* (2014) PHY-Layer Resiliency in OFDM Communications: A Tutorial. *IEEE Communications Surveys & Tutorials*, **17**, 292-314. https://doi.org/10.1109/COMST.2014.2349883

[4] Wei, X., Wang, Q., Wang, T. and Fan, J. (2016) Jammer Localization in Multi-Hop Wireless Network: A Comprehensive Survey. *IEEE Communications Surveys & Tutorials*, **19**, 765-799. https://doi.org/10.1109/COMST.2016.2631146

[5] Lichtman, M., Jover, R.P., Labib, M., Rao, R., Marojevic, V. and Reed, J.H. (2016) LTE/LTE-A Jamming, Spoofing, and Sniffing: Threat Assessment and Mitigation. *IEEE Communications Magazine*, **54**, 54-61.

https://doi.org/10.1109/MCOM.2016.7452266

[6] Borio, D., Dovis, F., Kuusniemi, H. and Presti, L.L. (2016) Impact and Detection of GNSS Jammers on Consumer Grade Satellite Navigation Receivers. *Proceedings of the IEEE*, **104**, 1233-1245. https://doi.org/10.1109/JPROC.2016.2543266

[7] Qin, W., Gamba, M.T., Falletti, E. and Dovis, F. (2020) An Assessment of Impact of Adaptive Notch Filters for Interference Removal on the Signal Processing Stages of a GNSS Receiver. *IEEE Transactions on Aerospace and Electronic Systems*, **56**, 4067-4082. https://doi.org/10.1109/TAES.2020.2990148

[8] Zhang, Y.D. and Amin, M.G. (2012) Anti-Jamming GPS Receiver with Reduced Phase Distortions. *IEEE Signal Processing Letters*, **19**, 635-638. https://doi.org/10.1109/LSP.2012.2209873

[9] Lu, D., Wu, R. and Liu, H. (2013) Global Positioning System Anti-Jamming Algorithm Based on Period Repetitive CLEAN. *IET Radar, Sonar & Navigation*, **7**, 164-169. https://doi.org/10.1049/iet-rsn.2010.0353

[10] Wu, J., Tang, X., Li, Z., Li, C. and Wang, F. (2019) Cascaded Interference and Multipath Suppression Method Using Array Antenna for GNSS Receiver. *IEEE Access*, **7**, 69274-69282. https://doi.org/10.1109/ACCESS.2019.2918775

[11] Huang, L., Lu, Z., Xiao, Z., Ren, C., Song, J. and Li, B. (2022) Suppression of Jammer Multipath in GNSS Antenna Array Receiver. *Remote Sensing*, **14**, 350. https://doi.org/10.3390/rs14020350

[12] Chien, Y.-R. (2013) Hybrid Successive Continuous Wave Interference Cancellation Scheme for Global Positioning System Receivers. *The Journal of Engineering*, **2013**, 7-14. https://doi.org/10.1049/joe.2013.0005

[13] Lotz, T. (2008) Adaptive Analog-to-Digital Conversion and Pre-Correlation Interference Mitigation Techniques in a GNSS Receiver. Technical University of Kaiserslautern, Kaiserslautern.

[14] Balaei, A.T. and Dempster, A.G. (2009) A Statistical Inference Technique for GPS Interference Detection. *IEEE Transactions on Aerospace and Electronic Systems*, **45**, 1499-1511. https://doi.org/10.1109/TAES.2009.5310313

[15] Cho, N.I. and Lee, S.U. (1993) On the Adaptive Lattice Notch Filter for the Detection of Sinusoids. *IEEE Transactions on Circuits and Systems II: Analog and Digital Signal Processing*, **40**, 405-416. https://doi.org/10.1109/82.238368

[16] Choi, J.W. and Cho, N.I. (2002) Suppression of Narrow-Band Interference in DS-Spread Spectrum Systems Using Adaptive IIR Notch Filter. *Signal Processing*, **82**, 2003-2013. https://doi.org/10.1016/S0165-1684(02)00385-7

[17] Xiao, Y., Takeshita, Y. and Shida, K. (2001) Steady-State Analysis of a Plain Gradient Algorithm for a Second-Order Adaptive IIR Notch Filter with Constrained Poles and Zeros. *IEEE Transactions on Circuits and Systems II: Analog and Digital Signal Processing*, **48**, 733-740. https://doi.org/10.1109/82.958344

[18] El Gebali, A. and Landry, R.J. (2022) Single and Multiple Continuous-Wave Interference Suppression Using Adaptive IIR Notch Filters Based on Direct-Form Structure in a QPSK Communication System. *Applied Sciences*, **12**, 2186. https://doi.org/10.3390/app12042186

[19] Chien, Y.-R., Huang, Y.-C., Yang, D.-N. and Tsao, H.-W. (2010) A Novel Continuous Wave Interference Detectable Adaptive Notch Filter for GPS Receivers. 2010 *IEEE Global Telecommunications Conference GLOBECOM*, Miami, 6-10 December 2010, 1-6. https://doi.org/10.1109/GLOCOM.2010.5684115

[20] Borio, D., Camoriano, L. and Presti, L.L. (2008) Two-Pole and Multi-Pole Notch

Filters: A Computationally Effective Solution for GNSS Interference Detection and Mitigation. *IEEE Systems Journal*, **2**, 38-47. https://doi.org/10.1109/JSYST.2007.914780

[21] Rusch, L.A. and Poor, H.V. (1994) Narrowband Interference Suppression in CDMA Spread Spectrum Communications. *IEEE Transactions on Communications*, **42**, 1969-1979. https://doi.org/10.1109/TCOMM.1994.583411

[22] Pashaian, M., Mosavi, M., Moghaddasi, M. and Rezaei, M. (2016) A Novel Interference Rejection Method for GPS Receivers. *Iranian Journal of Electrical and Electronic Engineering*, **12**, 9-20.

[23] Abbasi, M., Mosavi, M.R. and Reazei, M.J. (2020) GPS Continues Wave Jamming Canceller Using an ANF Combined with an Artificial Neural Network. 2020 8*th Iranian Joint Congress on Fuzzy and Intelligent Systems* (*CFIS*), Mashhad, 2-4 September 2020, 99-104. https://doi.org/10.1109/CFIS49607.2020.9238700

[24] El Gebali, A. and Landry, R. (2020) Mitigation of Continuous Wave Narrow-Band Interference in QPSK Demodulation Using Adaptive IIR Notch Filter. *American Journal of Signal Processing*, **10**, 10-18.

[25] Arif, S.W., Coskun, A. and Kale, I. (2020) A Novel Optimization Algorithm for Notch Bandwidth in Lattice Based Adaptive Filter for the Tracking of Interference in GPS. 2020 *IEEE International Symposium on Circuits and Systems* (*ISCAS*), Sevilla, 10-21 October 2020, 1-5. https://doi.org/10.1109/ISCAS45731.2020.9181117

[26] Stearns, S.D. (1985) Fundamentals of Adaptive Signal Processing. Sandia National Laboratories, Albuquerque.

[27] Ferdjallah, M. and Barr, R.E. (1994) Adaptive Digital Notch Filter Design on the Unit Circle for the Removal of Powerline Noise from Biomedical Signals. *IEEE Transactions on Biomedical Engineering*, **41**, 529-536. https://doi.org/10.1109/10.293240

[28] Choi, J.W. and Cho, N.I. (2001) Narrow-Band Interference Suppression in Direct Sequence Spread Spectrum Systems Using a Lattice IIR Notch Filter. 2001 *IEEE International Conference on Acoustics*, *Speech*, *and Signal Processing. Proceedings*, Vol. 4, 2237-2240.

[29] Shynk, J.J. (1989) Adaptive IIR Filtering. *IEEE ASSP Magazine*, **6**, 4-21. https://doi.org/10.1109/53.29644

[30] Regalia, P. (2018) Adaptive IIR Filtering in Signal Processing and Control. Routledge, London. https://doi.org/10.1201/9781315136653

[31] Nam Ik, C., Chong-Ho, C. and Sang Uk, L. (1989) Adaptive Line Enhancement by Using an IIR Lattice Notch Filter. *IEEE Transactions on Acoustics*, *Speech*, *and Signal Processing*, **37**, 585-589. https://doi.org/10.1109/29.17543

[32] Borio, D., Camoriano, L., Savasta, S. and Presti, L.L. (2008) Time-Frequency Excision for GNSS Applications. *IEEE Systems Journal*, **2**, 27-37. https://doi.org/10.1109/JSYST.2007.914914

[33] Chien, Y.-R. (2013) Design of GPS Anti-Jamming Systems Using Adaptive Notch Filters. *IEEE Systems Journal*, **9**, 451-460. https://doi.org/10.1109/JSYST.2013.2283753

[34] Arif, S.W., Coskun, A. and Kale, I. (2019) A Fully Adaptive Lattice-Based Notch Filter for Mitigation of Interference in GPS. 2019 15*th Conference on PhD Research in Microelectronics and Electronics* (*PRIME*), Lausanne, 15-18 July 2019, 217-220. https://doi.org/10.1109/PRIME.2019.8787822

[35] Lv, Q. and Qin, H. (2020) General Method to Mitigate the Continuous Wave Inter-

ference and Narrowband Interference for GNSS Receivers. *IET Radar*, *Sonar & Navigation*, **14**, 1430-1435. https://doi.org/10.1049/iet-rsn.2020.0115

[36] Lv, Q. and Qin, H. (2018) A Novel Algorithm for Adaptive Notch Filter to Detect and Mitigate the CWI for GNSS Receivers. 2018 *IEEE* 3*rd International Conference on Signal and Image Processing* (*ICSIP*), Shenzhen, 13-15 July 2018, 444-451. https://doi.org/10.1109/SIPROCESS.2018.8600453

[37] Same, M.H., Gleeton, G., Gandubert, G., Ivanov, P. and Landry, R. (2021) Multiple Narrowband Interferences Characterization, Detection and Mitigation Using Simplified Welch Algorithm and Notch Filtering. *Applied Sciences*, **11**, 1331. https://doi.org/10.3390/app11031331

[38] El Gebali, A. and Landry, R. (2021) Multi-Frequency Interference Detection and Mitigation Using Multiple Adaptive IIR Notch Filter with Lattice Structure. *Journal of Computer and Communications*, **9**, 58-77. https://doi.org/10.4236/jcc.2021.95005